Reduced Description of Complex Dynamics in Reactive Systems

Zhuyin Ren* and Stephen B. Pope

Sibley School of Mechanical & Aerospace Engineering, Cornell University, Ithaca, New York 14853

Received: March 5, 2007; In Final Form: June 25, 2007

Detailed chemical kinetics typically involve a large number of chemical species and a wide range of time scales. In calculations of chemically reactive flows, dimension-reduction techniques can be used to reduce the computational burden imposed by the direct use of detailed chemistry. In the reduced description, the reactive system is described in terms of a smaller number of reduced composition variables (e.g., some "major" species) instead of the full set of chemical species. Reactive flows exhibiting complex dynamics are especially challenging for dimension-reduction techniques and therefore provide more rigorous validation for such methods. Following the work of Brad et al. [*Proc. Combust. Inst.* **2007**, *31*, 455],[1] in this paper, we demonstrate the capability of the Invariant Constrained-equilibrium Edge Pre-Image Curve (ICE-PIC) dimension-reduction method [*J. Chem. Phys.* **2006**, *124*, Art. No. 114111][2] through calculations of the oxidation of a CO/H_2 mixture in a continuously stirred tank reactor (CSTR) at low pressure. The detailed chemical kinetics employed involves 11 species and 33 reactions. The system exhibits complex dynamics such as oscillatory ignition, oscillatory glow, and mixed mode oscillations. It is demonstrated that with five represented species the reduced description provided by the ICE-PIC method is able to quantitatively reproduce the observed complex dynamics. Moreover, the reduced description accurately predicts the boundaries of slow reaction, oscillatory ignition and the steady ignited state.

1. Introduction

Realistic modeling of chemically reactive systems, such as those describing atmospheric processes[3] and combustion,[4] involves a large number of chemical species, which participate in tens to thousands of elementary chemical reactions occurring simultaneously within a flow field. For example, the detailed mechanism for the primary reference fuels (iso-octane/*n*-heptane mixtures)[4] contains 1034 species which participate in 4326 elementary reactions. Consequently, typical reactive systems are modeled by a large set of partial differential equations (PDEs) representing the evolution of chemical species and energy, coupled with the flow fields. Besides the large number of chemical species involved, another challenging feature of chemical kinetics is the presence of a wide range of time scales, which adds dramatic computational burden and makes the direct use of detail chemical kinetics computationally expensive. However, it is essential somehow to incorporate the accurate chemical kinetics in calculations to reliably predict thermochemical quantities, especially for pollutants such as NO_x and particulates.[5]

For the reasons mentioned above, there is a well-recognized need to develop methods that radically reduce the computational burden imposed by the direct use of detailed chemical kinetics in modeling reactive systems. A great deal of work has focused on this effort, and it has been reviewed in several places.[6−8] One approach that is currently widely employed is the reduced description of reactive systems via dimension-reduction methods. The essential goal of dimension reduction is to describe reactive systems using a smaller number of reduced variables while reproducing the characteristics of the full description in which the full set of chemical species contained in the detailed kinetics is employed. One familiar dimension-reduction approach employs the quasi-steady-state assumption (QSSA)[9−12] wherein the fast "minor" species are assumed to be in quasi-steady state. Each of the resulting algebraic equations can be used to eliminate one minor species from the governing equations. In the reduced description, reactive systems are described in terms of only the "major" species. A reduced description obtained by dimension-reduction methods is based on the observation that, in general, the range of time scales for the chemical-kinetic processes is much larger than that for transport processes. Due to the fast chemical time scales, compositions in reactive flows quickly relax toward a low-dimensional manifold in the full composition space.[2,13−18] Therefore reactive systems can be well described along the low-dimensional attracting manifold with a smaller number of parametrization variables.

Over recent decades, a variety of dimension-reduction methods have been developed. Besides QSSA, other important methods include the Roussel & Fraser algorithm (RF),[14,15] rate-controlled constrained equilibrium (RCCE),[19,20] intrinsic low-dimensional manifolds (ILDMs),[16] trajectory-generated low-dimensional manifolds (TGLDM),[17] the computational singular perturbation (CSP),[21] the method of invariant manifolds,[22] the zero derivative principle method,[23,24] the invariant constrained-equilibrium edge pre-image curve (ICE-PIC) method,[2] the Davis algorithm,[25,26] and some variants of the above methods.[18,27,28] Most of the existing methods such as QSSA, RCCE, and ICE-PIC are developed on the basis of a transient homogeneous reactive system in the absence of transport processes such as convection, molecular diffusion and inflow/outflow.

To illustrate the ideas involved, we consider a homogeneous adiabatic, isobaric system with constant pressure P and enthalpy h. The system at time t is fully described by the full composition $\mathbf{z}(t)$, which can be taken to be the mass fractions of the n_s

* Corresponding author. E-mail: zr26@cornell.edu. Phone: (607) 255-3923. Fax: (607) 255-1222.

10.1021/jp0717950 CCC: $37.00
Published on Web 08/09/2007

species, or the species specific moles (mass fractions divided by the corresponding species molecular weights). Due to chemical reactions, the system evolves by the autonomous ordinary differential equations (ODEs)

$$\frac{d\mathbf{z}(t)}{dt} = \mathbf{S}(\mathbf{z}(t)) \tag{1}$$

where $\mathbf{S}$ is the rate of change of the composition given by the detailed chemical kinetics. The time-dependent solution to eq 1 corresponds to a reaction trajectory in the composition space which eventually relaxes to chemical equilibrium. Due to the fast time scales in the chemical kinetics, all the reaction trajectories quickly relax toward a low-dimensional attracting manifold in the composition space.[2,13−18] For the methods based on such homogeneous systems, the manifolds explicitly or implicitly identified (as approximations to the low-dimensional attracting manifold) by dimension-reduction methods are referred to as "chemistry-based", because they are identified solely on the basis of chemical kinetics without accounting for transport processes.

As shown in refs 29−33, the use of chemistry-based manifolds (or dimension-reduction methods) is suitable for describing inhomogeneous reactive flows with transport processes only when the chemical kinetics have a much wider range of time scales than do the transport processes. The implication of transport processes on the reduced description via "chemistry-based" manifolds (or "chemistry-based" dimension-reduction methods) is extensively studied in the literature such as refs 21, 29, 30−36, 38.

The manifold identified by dimension reduction can be parametrized by a smaller number of reduced composition variables; and, in the reduced description, the reactive system is described in terms of these reduced variables. To each reduced composition, there is a corresponding full composition on the manifold in the composition space. This process of determining the full composition from the reduced composition is termed "species reconstruction".[39]

The reduced description of reactive flows via dimension reduction has been increasingly applied in the numerical modeling of combustion processes such as laminar and turbulent flames.[7] For example in ref 40, a QSSA reduced mechanism for methane oxidation, which involves 19 species, is incorporated into calculations to predict NO_x and CO emissions in a turbulent flame. However, it is essential to validate the accuracy of the reduced description through the comparison with the full description (without reduction). In the combustion community, canonical tests include one-dimensional premixed laminar flames and autoignition of fuel/air mixtures. The validation of dimension-reduction methods can be achieved in terms of measuring local error and/or global error. In local error measurement, given a full composition from the full description, the corresponding reduced composition can be extracted and a reconstructed full composition can be obtained via species reconstruction; and comparison is made between the two full compositions in terms of compositions themselves as well as some dynamic quantities such as the rate-of-change vector. In global error measurement, comparisons are made between the reduced and full descriptions in terms of predictions for the dynamics and evolution of the reactive systems (in terms of species profiles, for example), or in terms of predictions of some global quantities such as flame speed or ignition delay time. Often, dimension-reduction methods are developed with local error control, and hence, the local error of the reduced description is in general well controlled. In most cases, if the local error is well controlled over a sufficiently wide range of conditions, the resulting dimension-reduction methods can be effectively used to describe reactive flows with well-controlled global error. However, as demonstrated by Brad et al.,[1] in the reduced description of reactive systems exhibiting complex dynamics, complex relationships can exist between the local and global errors: small local differences can lead to large deviations in the prediction of some global quantities such as ignition delay time and oscillatory periods. Hence, reactive systems exhibiting complex dynamics are particularly challenging for dimension-reduction methods and therefore provide a more rigorous validation.

Inspired by the recent work of Brad et al.,[1] in this study, we investigate the ICE-PIC dimension-reduction method[2] for the reduced description of reactive flows exhibiting complex dynamics, specifically the oxidation of a CO/H_2 mixture in a continuously stirred tank reactor (CSTR) at low pressure. The ICE-PIC method is recently developed by Ren et al.[2] for the reduced description of reactive flows based on spatially homogeneous systems in the absence of any transport processes. The low-dimensional manifold (called the ICE manifold) is an invariant trajectory-generated manifold. In addition, the ICE-PIC method provides a local species reconstruction technique which locally determines compositions on the ICE manifold without the need to generate the whole (or significant portions) of the ICE manifold. Compared to other dimension-reduction methods such as QSSA, RCCE and ILDM, the ICE-PIC method has the advantages of being based on an invariant manifold that is guaranteed to exist and to be continuous. This method is the first approach that locally determines compositions on a low-dimensional invariant manifold. Because it is local, the ICE-PIC method can readily be applied to high-dimensional reactive systems.

In the reduced description provided by the ICE-PIC method, the system is described by n_r reduced composition variables $\mathbf{r} = \{r_1, r_2, \cdots, r_{n_r}\}$ (with $n_r < n_s$), which are taken to be the specific moles of some user-specified "represented" species, and the specific moles of elements in the unrepresented species. (The specific moles of elements is a vector of length n_e, with n_e being the number of chemical elements in the system. The elements in the unrepresented species can be considered as "notional" species in the reduced description.) In general, the reduced composition $\mathbf{r}$ can be expressed as

$$\mathbf{r} = \mathbf{B}^{T}\mathbf{z} \tag{2}$$

where $\mathbf{B}$ is an $n_s \times n_r$ constant matrix. For example, if a component of $\mathbf{r}$ is a specified "major" species, then the corresponding column of $\mathbf{B}$ is a unit vector consisting of a single entry (unity) in the row corresponding to the major species. Full compositions on the ICE manifold are denoted by $\mathbf{z}^{ICE}(\mathbf{r},P,h)$. In applying the reduced description provided by the ICE-PIC method to general reactive flow problems, the full compositions are assumed to be on (or close to) the n_r-dimensional chemistry-based ICE manifold, i.e.,

$$\mathbf{z} = \mathbf{z}^{ICE}(\mathbf{r},P,h) \tag{3}$$

From the species reconstruction perspective, the accuracy of the ICE-PIC method has been examined in the autoignition and one-dimensional laminar flames of hydrogen/air and methane/air mixtures.[2,34] Those studies demonstrate that the local errors incurred by ICE-PIC, i.e., the errors in the reconstructed composition or the rate-of-change vector, are well controlled. In this study, for the first time, we demonstrate the application of the ICE-PIC method for the reduced description of reactive flows. In the reduced description, a set of governing equations for the reduced compositions is solved with the ICE-PIC method being used to perform species reconstruction and to evaluate the rate-of-change of the reduced compositions whenever necessary. This study serves to examine the accuracy of the ICE-PIC method in controlling the global errors by comparing the predictions from the reduced and full descriptions. It is shown that the reduced description provided by the ICE-PIC method is capable of quantitatively reproducing the complex dynamics exhibited in a continuously stirred tank reactor.

The paper is organized as follows: in section 2, the continuously stirred tank reactor is briefly described; in section 3, the reduced description by the ICE-PIC method is formulated; in section 4, the accuracy in the reduced description provided by the ICE-PIC method is examined; and conclusions are drawn in section 5.

2. Model Description

The system considered is the reaction of a $CO/H_2/O_2$ mixture in an isobaric continuously stirred tank reactor. As shown in refs 1 and 41−45, the dynamics exhibited by this system can be complex: the reaction may support five different modes of response (namely, steady slow reaction, steady flow, oscillatory glow, oscillatory ignition, and a steady ignited state) and therefore provides a good benchmark for investigating dimension-reduction methods. The focus of this study is not on the experimental or theoretical aspects of the complex dynamics exhibited in a CSTR, a thorough review of which is given in ref 45. Instead, we focus on investigating the capability of the ICE-PIC method to describe the complex dynamics exhibited by the CSTR.

The detailed chemical-kinetics mechanism employed for CO + H_2 oxidation is the CO + H_2 subset of the Leeds methane mechanism,[46,47] which involves 11 species and 33 reactions. The chemical species are H_2, O_2, H_2O, H_2O_2, CO, CO_2, H, O, OH, HO_2, and HCO. This detailed mechanism is the same as that used in ref 1, except that the absent inert species N_2 and Ar are removed. It is shown in ref 1 that this detailed chemical mechanism is capable of reproducing the complex dynamic exhibited by a CSTR over a range of pressures, reactor residence times and ambient temperatures. In the following study, comparisons are made between the full and reduced descriptions of the CSTR, i.e., directly using the detailed mechanism, and using ICE-PIC, respectively.

The reactive system at time t is fully described by $\{h(t), \mathbf{z}(t)\}$, where $h(t)$ is the specific enthalpy, and the full composition $\mathbf{z}(t)$ is taken to be the species specific moles. (The pressure P is fixed and is not shown explicitly in the notation.) With the assumption of perfect mixing in the reactor, the dynamics in a nonadiabatic CSTR are governed by the following set of ordinary differential equations (ODEs):

$$\frac{d\mathbf{z}}{dt} = \frac{\mathbf{z}^{in} - \mathbf{z}}{t_{res}} + \mathbf{S}(\mathbf{z},h)$$

$$\frac{dh}{dt} = \frac{h^{in} - h}{t_{res}} + (T_a - T(\mathbf{z},h))Q/\rho(\mathbf{z},h) \qquad (4)$$

where $\mathbf{z}^{in}$ and h^{in} are the species specific moles and enthalpy of the inflowing stream, t_{res} is the residence time, T_a is the ambient temperature, Q is the heat loss coefficient, T is the temperature in the reactor, and ρ is the density of the mixture in the reactor, and the vector $\mathbf{S}$ (determined by the detailed chemical kinetics)

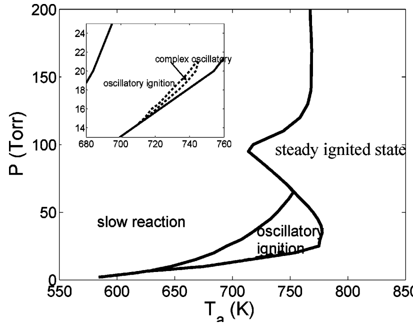

Figure 1. Regime diagram in the $P-T_a$ plane for the CSTR showing regions of slow reaction, simple and complex oscillatory ignition, and steady ignited state.

is the rate of change of the composition due to chemical reactions. As indicated by the notation, T, ρ, and $\mathbf{S}$ are known functions of $\mathbf{z}$ and h. A particular CSTR problem is determined by the specification of the parameters t_{res}, $\mathbf{z}^{in}$, h^{in}, P, T_a, and Q, and also by the initial conditions $\mathbf{z}(t=0)$ and $h(t=0)$. Tests are reported below for different values of P and T_a. All other parameters are fixed as follows: the heat loss coefficient Q is taken to be 160 J K^{-1} m^{-3} s^{-1} as in ref 1; the residence time is taken to be t_{res} = 8 s; the inflow mixture considered is 0.5% H_2, 49.5% CO, and 50% O_2 (by volume) at the ambient temperature T_a; the initial conditions are taken to be $\mathbf{z}(t=0) = \mathbf{z}^{in}$ with initial temperature $T(t=0)$ = 800 K. (The initial enthalpy $h(t=0)$ is determined from $\mathbf{z}(t=0)$ and $T(t=0)$.) The solution to eq 4 is obtained by integrating eq 4 forward in time by using the ODE solver DDASAC.[48]

Based on numerical solutions of eq 4 using the detailed mechanism, Figure 1 is a regime diagram in the $P-T_a$ plane showing the regions of slow reaction, simple and complex oscillatory ignition, and steady ignited state. As shown, at sufficiently low ambient temperature T_a no ignition occurs, and after an initial transient, the reactor exhibits a steady state with slow reaction. If the pressure in the reactor exceeds approximately 65 Torr, then crossing the ignition limit by increasing the ambient temperature causes the system to jump to a steady ignited state corresponding to a steady, high consumption of the incoming reactants, in which the concentrations of CO and H_2 in the reactor are very small. However, the transition at a lower pressure (P less than 65 Torr) is dynamically more complex. The reactor again exhibits a steady state with slow reaction at sufficiently low T_a. As T_a increases, the system passes into a region where sustained oscillation occurs. As shown in Figure 2, the system exhibits a periodic sequence of ignition events separated by periods of relatively little chemical activity, but during which the mixture composition changes under the influence of the inflow and outflow. If the ambient temperate is raised so that the system is taken further into the ignition region, the frequency of the oscillation increases (see Figure 11, below) and its magnitude decreases. For T_a sufficiently high, the amplitude decreases to zero and a steady ignited state emerges.

Brad et al.[1] performed a study of several existing reduction methods for the reduced descriptions of the oxidation of CO and H_2 in a CSTR. Two successful reduced descriptions were reported. In the first one, starting from the detailed mechanism, Brad et al. first developed a skeletal mechanism using sensitivity analysis to remove the unimportant reactions and species; then, on the basis of the skeletal mechanism, by employing quasi-steady-state assumptions, a QSSA reduced mechanism with seven major species was developed. In the second reduced description considered by Brad et al., a suitable data set was

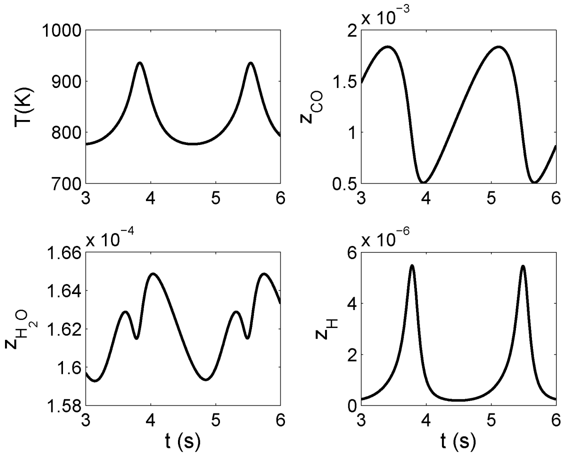

Figure 2. Temperature and specific moles (kmol/kg) of CO, H_2O, and H during oscillatory ignition (after the initial transient) for $T_a = 760$ K and $P = 25$ Torr.

generated from a wide range of temperatures, pressures and mixture compositions, by integrating the system of differential equations with the detailed chemical kinetics from a variety of initial conditions chosen to include all behavioral properties of the system. Then a final reduced description of only four variables (three represented species and an energy variable) was developed by fitting orthonormal polynomials to the generated data set.

In this study we investigate the recently developed ICE-PIC dimension-reduction method for the reduced description of the oxidation of CO and H_2 in a CSTR. The reduced description is given by the ICE-PIC method alone (without combination with other methods).

2.1. Strang Splitting Scheme. As mentioned earlier, the solution to eq 4 can be obtained by integrating eq 4 forward in time by using the ODE solver DDASAC.[48] In the following we introduce two splitting schemes for solving eq 4. The purpose is to isolate reaction from the inflow/outflow process so that the ICE-PIC method can be straightforwardly applied for the CSTR as shown in section 3. The two schemes now described are referred to as the "Strang scheme" and the "modified Strang scheme".

In the Strang splitting scheme,[37] eq 4 is integrated over a time step Δt as follows:

•Step 1. The reaction terms are integrated over a time interval $\Delta t/2$ by solving

$$\frac{d\mathbf{z}^a}{dt} = \mathbf{S}(\mathbf{z}^a, h^a)$$
$$\frac{dh^a}{dt} = 0 \tag{5}$$

The initial condition $\{\mathbf{z}^a(0), h^a(0)\}$ is taken to be the final state $\{\mathbf{z}, h\}$ from the previous step. This stiff system of equations is integrated over the time interval $\Delta t/2$ using the ODE solver DDASAC to yield $\{\mathbf{z}^a(\Delta t/2), h^a(\Delta t/2)\}$. The temperature and density after this substep are denoted by $T^a(\Delta t/2)$ and $\rho^a(\Delta t/2)$.

•Step 2. The inflow/outflow terms are integrated over a time interval Δt (using DDASAC) by solving

$$\frac{d\mathbf{z}^b}{dt} = \frac{\mathbf{z}^{in} - \mathbf{z}^b}{t_{res}}$$
$$\frac{dh^b}{dt} = \frac{h^{in} - h^b}{t_{res}} + (T_a - T(\mathbf{z}^b, h^b))Q/\rho(\mathbf{z}^b, h^b) \tag{6}$$

The initial conditions correspond to the final state of the system from the previous substep, $\{\mathbf{z}^a(\Delta t/2), h^a(\Delta t/2)\}$, and the solution to eq 6 is denoted by $\{\mathbf{z}^b(\Delta t), h^b(\Delta t)\}$.

•Step 3. A substep identical to step 1 is performed taking as the initial conditions the final state of the system from step 2, $\{\mathbf{z}^b(\Delta t), h^b(\Delta t)\}$. At the completion of this substep, the final state of the system is given by $\{\mathbf{z}^c(\Delta t/2), h^c(\Delta t/2)\}$. This serves as the initial condition for the next step.

In each of the three substeps, the ODEs are integrated accurately using DDASAC so that (over the range of Δt considered) the only significant numerical error is the splitting error (which is of order Δt^2).

The second scheme considered, namely the modified Strang scheme, is now described. The modification is, in step 2, to replace the accurate solution of eq 6 by a more simply computed second-order accurate solution obtained from the following predictor-corrector scheme.

•Predictor. The predictor for eq 6 is obtained by integrating over a time interval Δt by solving

$$\frac{d\mathbf{z}^b}{dt} = \frac{\mathbf{z}^{in} - \mathbf{z}^b}{t_{res}}$$
$$\frac{dh^b}{dt} = \frac{h^{in} - h^b}{t_{res} + (T_a - T^a(\Delta t/2))Q/\rho^a(\Delta t/2)} \tag{7}$$

where temperature $T^a(\Delta t/2)$ and density $\rho^a(\Delta t/2)$ are fixed to be the values obtained after step 1. Equation 7 is a set of uncoupled linear equations for which there are simple analytical solutions. The initial conditions correspond to the final state of the system from the previous substep, $\{\mathbf{z}^a(\Delta t/2), h^a(\Delta t/2)\}$ and the solution to eq 7 is denoted by $\{\mathbf{z}^p(\Delta t), h^p(\Delta t)\}$. The temperature and density obtained from $\{\mathbf{z}^p(\Delta t), h^p(\Delta t)\}$ are denoted by T^p and ρ^p, respectively.

•Corrector. The corrector for eq 6 is then obtained by integrating over a time interval Δt by solving

$$\frac{d\mathbf{z}^b}{dt} = \frac{\mathbf{z}^{in} - \mathbf{z}^b}{t_{res}}$$
$$\frac{dh^b}{dt} = \frac{h^{in} - h^b}{t_{res}} + \frac{1}{2}[(T_a - T^a(\Delta t/2))Q/\rho^a(\Delta t/2) + (T_a - T^p)Q/\rho^p] \tag{8}$$

The initial conditions correspond to the final state of the system from the previous substep, $\{\mathbf{z}^a(\Delta t/2), h^a(\Delta t/2)\}$, and the solution to eq 8 is denoted by $\{\mathbf{z}^b(\Delta t), h^b(\Delta t)\}$, which is the final state of the system after step 2.

The numerical errors in the two splitting schemes for solving eq 4 depend on the time step Δt. Given a prescribed accuracy, one needs to determine the required time step Δt that satisfies the accuracy. We define

$$\epsilon_T(\Delta t) \equiv \frac{1}{T_{DI}^{max}} \frac{1}{t_{end}} \int_0^{t_{end}} |T_{DI}(t) - T_{SP}(t, \Delta t)|\, dt \tag{9}$$

to be the measure of the error between the accurate solution $T_{DI}(t)$ from the direct integration of the full coupled equations

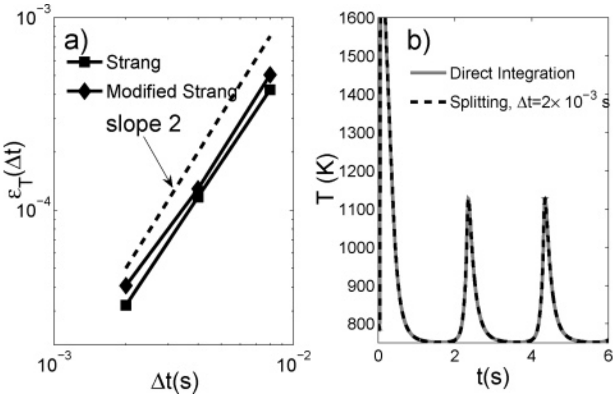

Figure 3. Demonstration of the accuracy of the Strang splitting scheme and the modified Strang splitting scheme for the oscillatory ignition with $T_a = 750$ K and $P = 25$ Torr. (a) Splitting error defined by eq 9 against time step Δt. Also shown are the dashed line of slope 2 corresponding to second-order accuracy ($\epsilon_T(\Delta t) \sim \Delta t^2$). (b) Comparison between the accurate direct integration of eq 4 and the modified Strang splitting scheme (see section 3.1) with time step $\Delta t = 2 \times 10^{-3}$ *s*.

(eq 4), and the solution $T_{SP}(t,\Delta t)$ from one of the splitting schemes with time step Δt, where T_{DI}^{max} is the maximum temperature (after the initial transient) from the accurate solution. (For the results presented below $t_{end} = 4$ s.) Figure 3 shows the numerical errors ϵ_T against the time step Δt during the oscillatory ignition with $T_a = 750$ K and $P = 25$ Torr. As shown in the plot, the error decreases with Δt, essentially as Δt^2, thus illustrating the second-order accuracy of both the Strang splitting scheme and the modified Strang splitting scheme. The predictor-corrector method employed for the inflow/outflow process in the modified scheme preserves the second-order accuracy of the Strang splitting scheme, and, in the tests performed, incurs an additional error of less than 30%. With $\Delta t = 2 \times 10^{-3}$ s, the splitting error in the modified Strang scheme is about 4×10^{-5}. As shown in Figure 3b, there are no noticeable differences between the solutions from the direct integration of the full coupled equations (eq 4) and from the modified Strang splitting system with $\Delta t = 2 \times 10^{-3}$ s. On the basis of this study, the time step $\Delta t = 2 \times 10^{-3}$ s is employed in all the numerical results reported below.

A more complete study of splitting schemes suitable for use with ICE-PIC and other chemistry-based manifolds is described in ref 49.

3. Reduced Description of a CSTR by the ICE-PIC Method

With a specified reduced representation $\mathbf{r} = \mathbf{B}^T\mathbf{z}$ (i.e., with a specified matrix $\mathbf{B}$) the exact (but unclosed) reduced description for the CSTR with constant pressure P can be obtained by pre-multiplying eq 4 with $\mathbf{B}^T$

$$\frac{d\mathbf{r}}{dt} = \mathbf{B}^T\mathbf{S}(\mathbf{z},h) + \frac{\mathbf{r}^{in} - \mathbf{r}}{t_{res}}$$
$$\frac{dh}{dt} = \frac{h^{in} - h}{t_{res}} + (T_a - T(\mathbf{z},h))Q/\rho(\mathbf{z},h) \qquad (10)$$

where $\mathbf{r}^{in} \equiv \mathbf{B}^T\mathbf{z}^{in}$, and temperature T, density ρ, and $\mathbf{S}$ are functions of $\mathbf{z}$ and h. Equation 10 is unclosed because $\mathbf{z}(t)$, which is not known exactly in terms of $\mathbf{r}(t)$ and $h(t)$, is needed for evaluating temperature, density, and $\mathbf{S}$. To close this set of equations, dimension-reduction methods are used, which introduce assumptions or approximations. In the reduced description provided by the ICE-PIC method, the full compositions are assumed to be on the n_r-dimensional chemistry-based ICE manifold, i.e.,

$$\mathbf{z}(t) = \mathbf{z}^{ICE}(\mathbf{r}(t),h(t)) \qquad (11)$$

(In this study, we neglect departures of the composition from the manifold, which may be introduced by the inflow/outflow processes. For the reduced description with relatively high dimensionality, based on the results shown below, this approximation is satisfactory.) Hence, the governing equations for the reduced composition are

$$\frac{d\mathbf{r}}{dt} = \mathbf{B}^T\mathbf{S}(\mathbf{z}^{ICE}(\mathbf{r},h),h) + \frac{\mathbf{r}^{in} - \mathbf{r}}{t_{res}} = \mathbf{S}_r(\mathbf{r},h) + \frac{\mathbf{r}^{in} - \mathbf{r}}{t_{res}}$$
$$\frac{dh}{dt} = \frac{h^{in} - h}{t_{res}} + (T_a - T(\mathbf{z}^{ICE}(\mathbf{r},h),h))Q/\rho(\mathbf{z}^{ICE}(\mathbf{r},h),h) \qquad (12)$$

where the vector $\mathbf{S}_r(\mathbf{r},h) \equiv \mathbf{B}^T\mathbf{S}(\mathbf{z}^{ICE}(\mathbf{r},h),h)$ is of length n_r.

Similar to the modified Strang splitting scheme described in section 2.1, eq 12 for the reduced description provided by the ICE-PIC method is solved using the following splitting procedure:

•Step 1. The reduced composition is advanced over a time interval $\Delta t/2$ due to chemical reaction. The governing equations for this substep can be written as

$$\frac{d\mathbf{r}^a}{dt} = \mathbf{S}_r(\mathbf{r}^a,h^a)$$
$$\frac{dh^a}{dt} = 0 \qquad (13)$$

where $\mathbf{S}_r(\mathbf{r}^a,h^a)$ is a complicated function of $\mathbf{r}^a$ and h^a. By exploiting the fact that the ICE manifold is invariant, in the numerical implementation, this substep is performed though the following three steps:

(1) On the basis of the reduced composition from the previous step, perform species reconstruction to obtain the full composition on the ICE manifold $\{\mathbf{z}^{ICE}, h^{ICE}\}$. (In the numerical implementation, the full composition on the ICE manifold is obtained using Newton iterations. Its accuracy is determined by the pre-specified relative error control parameter ϵ.)

(2) Integrate eq 5 with the detailed mechanism over a time interval $\Delta t/2$ to obtain the full composition after reaction, $\{\mathbf{z}^R, h^R\}$. Other known quantities after the reaction substep are temperature T^R and density ρ^R.

(3) Extract the reduced composition after reaction $\{\mathbf{r}^a(\Delta t/2), h^a(\Delta t/2)\}$ from the full composition $\{\mathbf{z}^R, h^R\}$ through

$$\mathbf{r}^a(\Delta t/2) = \mathbf{B}^T\mathbf{z}^R$$
$$h^a(\Delta t/2) = h^R \qquad (14)$$

•Step 2. The predictor for the inflow/outflow process is obtained by integrating the following equations over a time interval Δt

$$\frac{d\mathbf{r}^b}{dt} = \frac{\mathbf{r}^{in} - \mathbf{r}^b}{t_{res}}$$
$$\frac{dh^b}{dt} = \frac{h^{in} - h^b}{t_{res}} + (T_a - T^R)Q/\rho^R \qquad (15)$$

where temperature T^R and density ρ^R are fixed (i.e., the values obtained after the previous reaction substep). Equation 15 is a set of uncoupled linear equations for which there are simple analytical solutions. The initial conditions correspond to the final state of the system from the previous reaction substep, $\{\mathbf{r}^a(\Delta t/2), h^a(\Delta t/2)\}$, and the solution to eq 15 is denoted by $\{\mathbf{r}^p(\Delta t), h^p(\Delta t)\}$. A species reconstruction is then performed to obtain the temperature T^p and density ρ^p on the ICE manifold point corresponding to $\{\mathbf{r}^p(\Delta t), h^p(\Delta t)\}$. The corrector is then obtained by integrating over a time interval Δt by solving

$$\frac{d\mathbf{r}^b}{dt} = \frac{\mathbf{r}^{in} - \mathbf{r}^b}{t_{res}}$$

$$\frac{dh^b}{dt} = \frac{h^{in} - h^b}{t_{res}} + \frac{1}{2}[(T_a - T^R)Q/\rho^R + (T_a - T^p)Q/\rho^p] \quad (16)$$

The initial conditions correspond to the final state of the system from the previous reaction substep, $\{\mathbf{r}^a(\Delta t/2), h^a(\Delta t/2)\}$, and the solution to eq 16 is denoted by $\{\mathbf{r}^b(\Delta t), h^b(\Delta t)\}$, which is the final state of the system after step 2.

•Step 3. A substep identical to step 1 is performed by taking as the initial conditions the final state of the system from step 2, $\{\mathbf{r}^b(\Delta t), h^b(\Delta t)\}$. At the completion of this substep, the final state of the system is given by $\{\mathbf{r}^c(\Delta t), h^c(\Delta t/2)\}$. This serves as the initial condition for the next step.

4. Results and Discussions

4.1. Dimension Analysis. Before applying the ICE-PIC method for the reduced description of the oxidation of CO and H_2 in a CSTR, one has to determine the necessary dimension for an accurate reduced description of the observed dynamics. In this study, this is achieved on the basis of time scale analysis. The relevant quantity considered is the Jacobian matrix $\mathbf{J}$ ($n_s \times n_s$) of the reaction source term, which is defined as

$$J_{ij}(\mathbf{z}) \equiv \frac{\partial S_i}{\partial z_j} \quad (17)$$

For a reactive system, the eigenvalues of the Jacobian matrix of the reaction source term are related to the chemical time scales τ_i by $\tau_i = 1/|\lambda_i^r|$, where λ_i^r denotes the real part of the ith eigenvalue. Moreover, there are n_e eigenvalues that are exactly zero due to the conservation of elements. Also the Jacobian matrix contains the information that describes the short-time evolution of a small perturbation to the nonlinear chemical system.[7,16] For $\lambda_i^r > 0$, the magnitude of the perturbation increases; for $\lambda_i^r = 0$, the magnitude of the perturbation does not change with time; for $\lambda_i^r < 0$, the magnitude of the perturbation relaxes toward zero. A Jacobian matrix with a set of eigenvalues with large negative real parts implies the existence of a low-dimensional attracting manifold in the composition space. It is informative to look at some representative spectra of the eigenvalues of the Jacobian in the oxidation of CO and H_2 in a CSTR, which provide the characteristic chemical times scales.

Figures 4 and 5 show two representative spectra of eigenvalues along the oscillatory trajectories (solutions to eq 4) for the oxidation of CO and H_2 in a CSTR at two different ambient temperatures. The figures show the evolution of the real parts of the eigenvalues, which are either great than 1 s^{-1} or less than -1 s^{-1}. As may be seen from Figures 4 and 5, there are several large (in magnitude) negative eigenvalues even at low temperatures along the trajectories. The largest (in magnitude) negative eigenvalue (order of 10^6 s^{-1}, which implies that the fast chemical time scale is of order 10^{-6} s), is almost constant along the trajectories. At high temperatures along the trajectories, the number of small eigenvalues increases; i.e., the number of fast chemical time scales increases. Recall that the characteristic flow time scale in a CSTR is the residence time τ_{res} that is 8 s

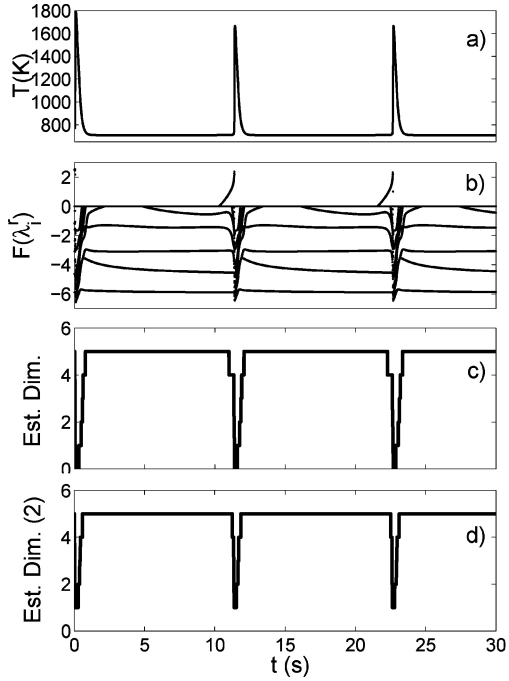

Figure 4. Chemical time scales and calculated manifold dimension during oscillatory ignition with $T_a = 710$ K and $P = 25$ Torr: (a) temperature along the trajectory; (b) real parts of the eigenvalues of the Jacobian matrix shown as $F(\lambda_i^r)$, where for $\lambda_i^r \le -1$, $F(\lambda_i^r) = -\log_{10}(\max(-\lambda_i^r,1))$, for $\lambda_i^r \ge 1$, $F(\lambda_i^r) = -\log_{10}(\max(\lambda_i^r,1))$, and for $-1 < \lambda_i^r < 1$, $F(\lambda_i^r) = 0$; (with λ_i^r being in inverse seconds) (c) estimated dimension based on time scale analysis; (d) estimated dimension based on the analysis of sensitivity matrices.

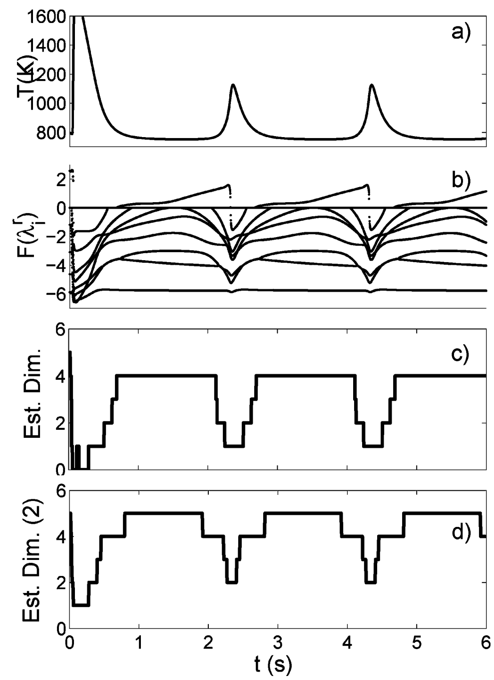

Figure 5. Chemical time scales and calculated manifold dimension during oscillatory ignition with $T_a = 750$ K and $P = 25$ Torr: (a) temperature along the trajectory; (b) real parts of the eigenvalues of the Jacobian matrix shown as $F(\lambda_i^r)$ (defined in Figure 4); (c) estimated dimension based on time scale analysis; (d) estimated dimension based on the analysis of sensitivity matrices.

for the cases considered. As may be seen from Figure 4, even for the case (T_a = 710 K), where the ambient temperature is close to the lower boundary of in the $P-T_a$ diagram (see Figure 1), some chemical time scales along the oscillatory trajectories are much smaller than the flow time scale.

Due to the small chemical time scales, it is reasonable to assume the existence of low-dimensional attracting manifolds in the full composition space, and a chemistry-based dimension-reduction method such as ICE-PIC is suitable for a reduced description of the system. In this study, two different methods are employed to study the required dimensionality for an accurate reduced description of the system. For the first method, the required dimensionality is estimated on the basis of simple time scale analysis, where the characteristic flow time τ_{res} can serve as the threshold value. The second method employed is the one developed by Ren and Pope[13] where the required dimensionality is obtained on the basis of the analysis of the sensitivity matrices. Figures 4 and 5 show the calculated necessary dimension for the reduced description along the trajectories. For the first method, it is obtained as $n_s - n_e - n_f$, where n_f is the number of fast chemical time scales (with negative corresponding eigenvalues) that are smaller than $0.002\tau_{res}$ at each point along the oscillatory ignition. For the second method, it is obtained through the following procedures:

•Starting from each full composition along the oscillatory ignition, follow the pure reaction trajectory (without inflow/outflow) and obtain the correspondingly sensitivity matrix after $0.002\tau_{res}$.

•For each full composition on the solution, determine its dimensionality based on the the singular values of the sensitivity matrices. The required dimensionality is defined to be the number of singular values that are greater than the threshold value, which is taken to be 0.01 in this study.

As may be seen from Figures 4 and 5, the necessary dimension fluctuates as the trajectories proceed, and the two methods provide consistent estimates. In the low-temperature regions, the required dimension is maximum, with considerably lower dimension occurring near peaks in temperature. This is due to the fast chemical processes at high temperatures as revealed by the larger (in magnitude) negative eigenvalues. On the basis of the dimension study, the highest estimated dimension required is five, over a wide range of ambient temperature T_a and pressure P. Hence, for most results shown below, the reduced description by the ICE-PIC method employs five represented species (plus three elements). This is a conservative estimate of the required dimensionality at high ambient temperatures. In fact, for high ambient temperatures, as shown below, a reduced description with a smaller number of represented species can accurately reproduce the complex dynamics.

One point worthy of mentioning is the required dimension for the reduced description at low temperatures along the solution trajectory for a CSTR. Figure 6 shows the magnitude of the reaction and inflow/outflow during the oscillatory ignition. As shown in the plot, the dominant physical process at low temperatures is the inflow/outflow with extremely slow chemical reactions. (The radical buildup during these extremely slow chemical reactions is essential to the observed dynamics.) At low temperatures, the evolution of composition **z** in the full composition space is well approximated by

$$\frac{d\mathbf{z}}{dt} \approx \frac{\mathbf{z}^{in} - \mathbf{z}}{t_{res}} \tag{18}$$

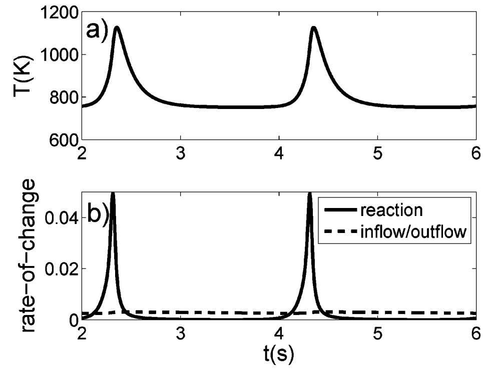

Figure 6. Magnitude (2-norm) of different physical processes during oscillatory ignition (after the initial transient) with T_a = 750 K and P = 25 Torr: (a) temperature along the trajectory; (b) magnitude of reaction, $|\mathbf{S}|$, and inflow/outflow, $|\mathbf{z}^{in} - \mathbf{z}|/\tau_{res}$ processes along the trajectory (units of mol kg^{-1} s^{-1}).

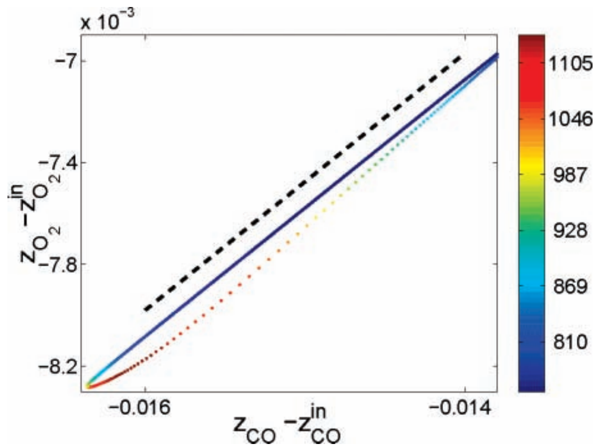

Figure 7. Projection onto the $CO-O_2$ plane of the trajectory during oscillatory ignition (after the initial transient) with T_a = 750 K and P = 25 Torr. The trajectory is colored by the corresponding temperature along the trajectory. Also shown for reference is a straight dashed line. Figure demonstrates that compositions in the low-temperature region lie close to a straight line.

The solution to eq 18 corresponds to a straight line in composition space, which is demonstrated in Figure 7. As long as at low temperatures chemical reactions are slow compared to inflow/outflow process, this is true no matter whether or not the system undergoes periodic oscillations. (For a system undergoing periodic oscillations, the trajectory in the composition space is a closed curve. Every period corresponds to traversing the curve once. Hence, it is inevitable that the compositions after the initial transient lie on a one-dimensional manifold (but not necessarily a straight line).) This does not contradict the observation based on time scale analysis: the required dimension for the reduced description is maximum at low temperatures (even though the compositions at low temperatures lie close to a one-dimensional manifold). The one-dimensional manifold, formed as a result of inflow/outflow process, is not attractive and cannot be described by a chemistry-based dimension-reduction method such as the ICE-PIC method with only one reduced variable. Nevertheless, this low-dimensional manifold at low temperatures (controlled by transport processes) may be exploited by fitting techniques such as repro-modeling, which are not used in this study.

4.2. Predictions of Complex Dynamics by ICE-PIC. Having determined the required dimension, in the following, we show the prediction of complex dynamics exhibited in a CSTR by the ICE-PIC method. One important aspect of the reduced description is the choice of the reduced representation, i.e., the

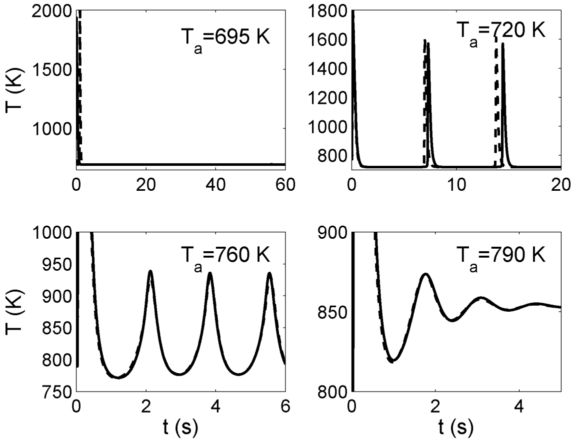

Figure 8. Comparison at different ambient temperatures T_a with $P = 25$ Torr between the full description (solid lines) and the reduced description (dashed lines) provided by the ICE-PIC method with H_2, O_2, CO, H, and O being the represented species.

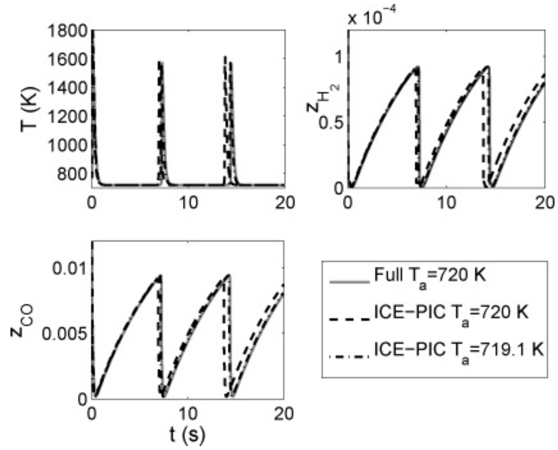

Figure 9. Temperature and specific moles (kmol/kg) of CO and H_2 for oscillatory ignition with $P = 25$ Torr. The figure illustrates that a small change in T_a brings the reduced description by ICE-PIC in line with the full description. Key: solid line, full description with $T_a = 720$ K; dashed line, reduced description with $T_a = 720$ K; dash-dotted line, reduced description with $T_a = 719.1$K.

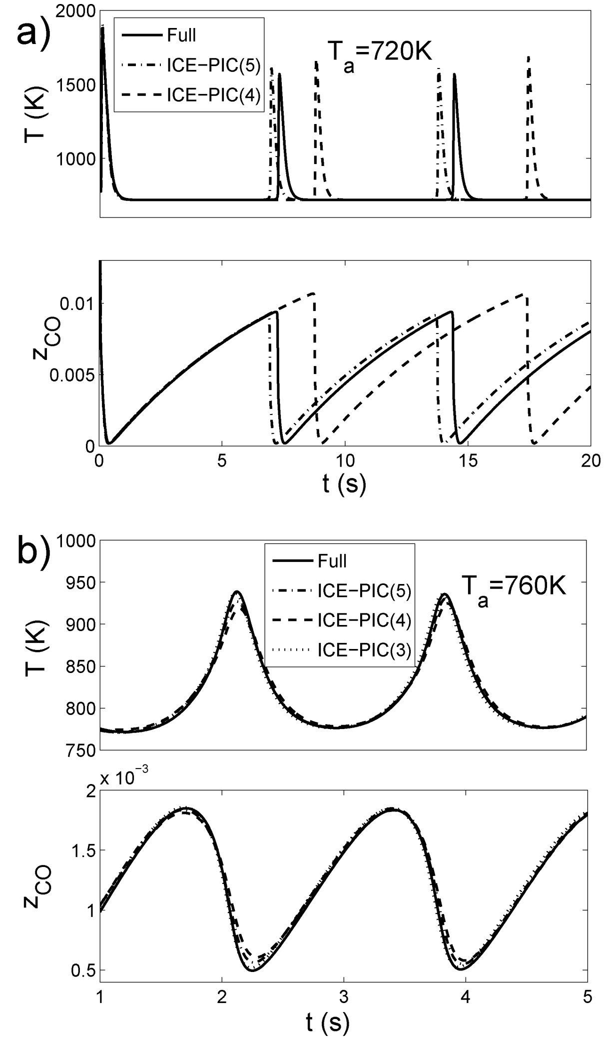

Figure 10. Effect of the dimensionality of the reduced description of the CSTR at different ambient temperatures with $P = 25$ Torr: solid line, full description; dash-dotted line, ICE-PIC with five represented species, i.e., H_2, O_2, CO, H, and O; dashed line, ICE-PIC with four represented species, i.e., H_2, CO, H, and O; dotted line, ICE-PIC with three represented species, i.e., H_2, CO, and O.

specification of n_r and **B**. In this study, we consider several different reduced representations, and the effects of which are shown below.

Figure 8 shows the predicted temperature profiles by the ICE-PIC method with H_2, O_2, CO, H, and O being the represented species at different ambient temperatures T_a. The reduced description successfully reproduces the dynamics in the regions of steady slow reaction, oscillatory ignition, and steady ignited state. For low temperatures (e.g., $T_a = 720$ K), close to the lower boundary of the oscillatory ignition (see Figure 1), the peak temperatures are well represented although there are small shifts in the periods of the oscillations. Although the difference between the reduced description and the full description at a particular time point seems large, as shown in Figure 9 it is eliminated by a small shift in the ambient temperature, indicating that the error relates to a small shift in the $P-T_a$ diagram. (This phenomenon is also observed by Brad et al.[1] for the QSSA method.) With increasing ambient temperature, the accuracy of the reduced description improves. This is due to the fact (see Figures 4 and 5) that, with increasing ambient temperature, the required dimensionality for the reduced description decreases. In fact, at high ambient temperatures, as shown in Figure 10, a reduced description with a smaller number of represented species can accurately reproduce the complex dynamics. In contrast, low ambient temperatures, a reduced description with a smaller number of represented species results in a significant shift in the phase and period of the oscillations.

An important quantity, which characterizes the oscillatory ignition, is the period of oscillation. Figure 11 shows the predictions for the period of oscillations from both the full and reduced descriptions. As shown in the plot, the dynamics of the system (e.g., the period of oscillation) is extremely sensitive to the ambient temperature. (This can be seen from the large slope (in magnitude) close to the lower boundary of the oscillatory region.) Nevertheless, the reduced description provided by the ICE-PIC method successfully reproduces the dynamics in terms of the period prediction in the whole oscillatory ignition region. The difference close to the lower boundary corresponds to a small shift in the ambient temperature. Moreover, the reduced description accurately predicts the region of oscillatory ignition. The predicted lower boundaries for the oscillatory ignition (with $P = 25$ Torr) from the full and reduced description are 696.2 and 694.9 K, respectively. The predicted upper boundaries are almost identical (with the difference being less than 0.1 K).

As pointed out by Brad et al.,[1] the extreme sensitivity of the dynamics close to the lower boundary of the oscillatory region

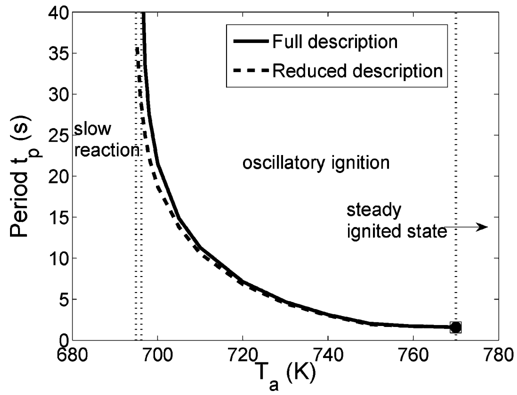

Figure 11. Variation of the period of oscillation t_p with ambient temperature T_a with $P = 25$ Torr in the CSTR: solid curve, prediction from full description; dashed curve, prediction from reduced description provided by the ICE-PIC method with H_2, O_2, CO, H, and O being the represented species; vertical dotted lines, predicted oscillatory ignition boundaries from the full and reduced descriptions (696.2 and 694.9 K, respectively for the lower boundary).

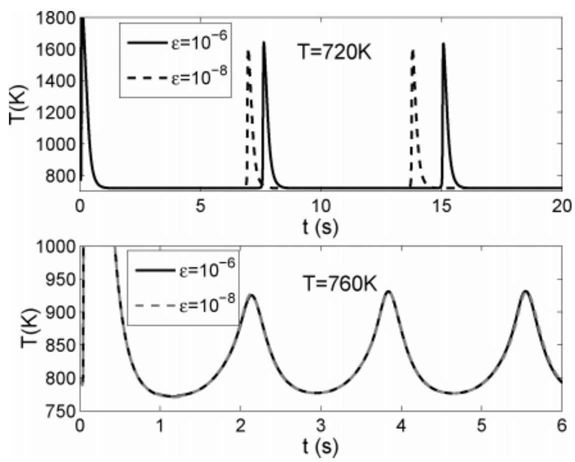

Figure 12. For different ambient temperatures T_a with $P = 25$ Torr, temperature against time from the reduced description of oscillatory ignition provided by the ICE-PIC method with different values of relative error control parameter ϵ in species reconstruction. In the reduced description, the represented species are H_2, O_2, CO, H, and O.

highlights the potential challenge for the reduced description: a small local error introduced in the reduced description can produce a very different dynamical behavior such as a large discrepancy in the period of oscillation. To demonstrate, here we show the effect of the numerical error (introduced by the ICE-PIC implementation in the reduced description) on the dynamics of the system. Figure 12 shows the predicted temperature from the reduced description of oscillatory ignition provided by the ICE-PIC method with different relative error control parameters ϵ in the species reconstruction. At high ambient temperatures (e.g., $T_a = 760$ K), the dynamics is relatively insensitive to the numerical error so that a relative large error tolerance can be employed. In contrast, for low temperatures (e.g., $T_a = 720$ K), the dynamics is extremely sensitive to the numerical error. A small local error introduced can be amplified and produce a very different dynamical behavior later. Hence, for low temperatures close to the lower boundary of the oscillatory region, a tight numerical error control is required. For the calculations presented in this paper, the error tolerance in the ICE-PIC method is specified as $\epsilon = 10^{-8}$, which is sufficiently small so that the incurred error in the reconstructed composition does not have a significant effect on the dynamics of the system. (For the above two ambient temperatures, there

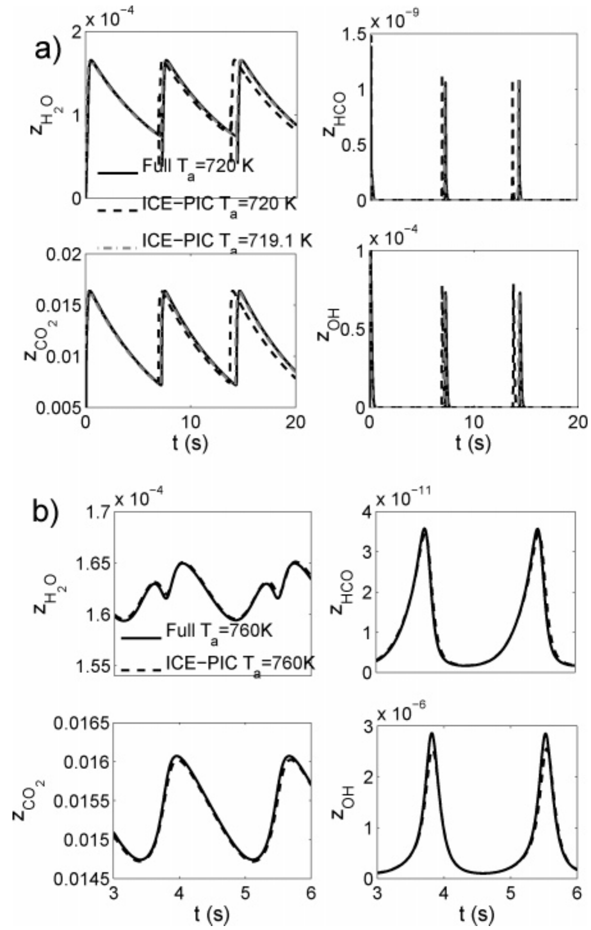

Figure 13. Reconstructed species specific moles (kmol/kg) for the unrepresented species in the ICE-PIC reduced description of the CSTR at different ambient temperature with $P = 25$ Torr. (a) $T_a = 720$ K. Also shown are the results from the reduced description with $T_a = 719.1$ K. (b) $T_a = 760$ K. Key: solid lines, predictions from full description; dashed (and dash-dotted) lines, prediction from the ICE-PIC method with H_2, O_2, CO, H, and O being the represented species.

are no observable difference between the dynamics of the system with $\epsilon = 10^{-8}$ and $\epsilon = 10^{-10}$.)

In the reduced description, only the represented species are known. However, whenever needed, the full composition (or the unrepresented species) can be obtained through species reconstruction. Figure 13 shows the reconstructed specific moles (kmol/kg) of the unrepresented species H_2O, CO_2, OH and HCO in the ICE-PIC reduced description at different ambient temperatures. As may be seen from the figure, all the reconstructed unrepresented species (even HCO with extremely low concentrations) agree well with the predictions from the full description. For low temperatures (e.g., $T_a = 720$ K), although the difference in the unrepresented species between the reduced description and the full description at a particular time point seems large, the difference is eliminated by a small shift in the ambient temperature as shown in Figure 13.

In the reduced description of reactive flows by dimension-reduction methods, one essential aspect is the choice of the reduced representation, e.g., the specification of the represented species. For example, in the QSSA method, the accuracy of the reduced description depends strongly on the successful identification of the fast QSSA species, which is still a challenging research area.[50] This is also the case for the RCCE method, as demonstrated in ref 51. For those dimension-reduction methods, obtaining a satisfactory reduced representation is still a challenging and sometimes an extremely tedious

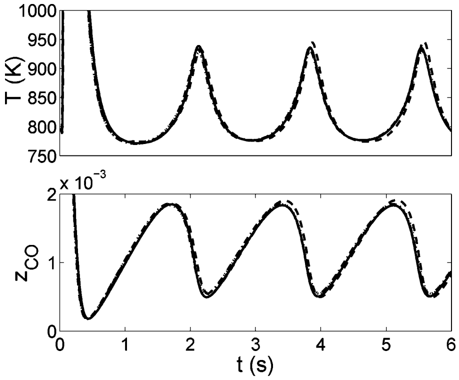

Figure 14. Effect of different choices of represented species on the reduced description of the CSTR with $T_a = 760$ K and $P = 25$ Torr: solid line, full description; dash-dotted line, ICE-PIC with H_2, O_2, H_2O, CO, and H being represented species; dotted line, ICE-PIC with H_2, O_2, CO, H, and O being represented species; dashed line, ICE-PIC with H_2, CO, H, O, and OH being represented species.

task. Nevertheless, the difficulty of choosing an appropriate reduced representation is alleviated in the ICE-PIC reduced description. Figure 14 shows the effect of different choices of represented species on the reduced description. Three different sets of represented species are employed, specifically {H_2, O_2, H_2O, CO, H}, {H_2, O_2, CO, H, O}, and {H_2, CO, H, O, OH}. As may be seen from the figure, the differences between the three reduced descriptions are small and they all agree well with the full description.

5. Conclusion

In this study, we demonstrate the application of the ICE-PIC method for the reduced description of reactive flows, specifically the oxidation of CO and H_2 in a continuously stirred tank reactor (CSTR). The system exhibits complex dynamics such as oscillatory ignition, oscillatory glow, and mixed mode oscillations, which are particularly challenging for dimension-reduction methods. The study reveals that, even at low temperatures along the oscillatory trajectories, there are several fast chemical times scales (order of 10^{-4} to 10^{-6} s), which are much faster than the characteristic flow time t_{res}. At high temperatures along the trajectories, the number of fast chemical time scales increases. Based on the observed fast chemical time scales, the study confirms that a chemistry-based dimension-reduction method such as ICE-PIC is suitable for a reduced description of the reactive system.

To implement the reduced description, an operator splitting scheme is used to separate reaction from other processes such as inflow/outflow, and a set of governing equations for the reduced compositions is obtained and solved. In the reaction substeps, the ICE-PIC method first performs species reconstruction to obtain the full composition on the ICE low-dimensional manifold; then the full composition after reaction is obtained by integrating the corresponding ODEs with full chemical kinetics; and finally, the reduced composition after reaction is obtained from the full composition.

The capability and accuracy of the ICE-PIC method is demonstrated through the calculations of the CSTR. This study, for the first time, demonstrates the accuracy of the ICE-PIC method in terms of controlling the global error by comparing the predictions from the reduced and full descriptions. It serves to significantly complement previous studies[2,34] where the accuracy of the ICE-PIC method in controlling local error is studied through species reconstruction.

For the chemical system considered, at low ambient temperatures (e.g., $T_a = 710$ K), the number of degrees of freedom (i.e., the required dimensionality for the reduced description) is five. With increasing ambient temperature, the required dimensionality for the reduced description decreases. For $T_a = 760$ K, as demonstrated, three represented species are sufficient to represent the system. It is shown that over a wide range of temperatures, with five represented species, the reduced description provided by the ICE-PIC method is able to quantitatively reproduce the complex dynamics exhibited by the CSTR. The reduced description accurately predicts the boundaries of slow reaction, oscillatory ignition and steady ignited state.

Moreover, the study shows that the differences between the reduced descriptions provided by the ICE-PIC method with different representations (i.e., with different specifications of the represented species) are small and they all agree well with the full description. Hence, the ICE-PIC method is not sensitive (to some extent) to the reduced representation. This is a significant advantage over other methods such as QSSA and RCCE, where the accuracy of the reduced description depends strongly on the reduced representation, and the successful specification of reduced representation is still a challenging research area.

The reduced description provided by ICE-PIC is at least as accurate as those reported by Brad et al.[1]

Acknowledgment. This research is supported by the National Science Foundation through Grant No. CBET-0426787. The authors would like to thank Dr. Alison Tomlin for providing the information on the *CO/H$_2$* mechanism.

References and Notes

(1) Brad, R. B.; Tomlin, A. S.; Fairweather, M.; Griffiths, J. F. *Proc. Combust. Inst.* **2007**, *31*, 455.
(2) Ren, Z.; Pope, S. B.; Vladimirsky, A.; Guckenheimer, J. M. *J. Chem. Phys.* **2006**, *124*, Art. No. 114111.
(3) Geiger, H.; Barnes, I.; Becker, K. H.; Bohn, B.; Brauers, T.; Donner, B.; Dorn, H.-P.; Elend, M.; Freitas Dinis, C. M.; Grossmann, D.; Hass, H.; Hein, H.; Hoffmann, A.; Hoppe, L.; Hülsemann, F.; Kley, D.; Klotz, B.; Libuda, H. G.; Maurer, T.; Mihelcic, D.; Moortgat, G. K.; Olariu, R.; Neeb, P.; Poppe, D.; Ruppert, L.; Sauer, C. G.; Shestakov, O.; Somnitz, H.; Stockwell, W. R.; Thüner, L. P.; Wahner, A.; Wiesen, P.; Zabel, F.; Zellner, R.; Zetzsch, C. *J. Atmos. Chem.* **2002**, *42*, 323.
(4) Curran, H. J.; Gaffuri, P.; Pitz, W. J.; Westbrook, C. K. *Combust. Flame* **2002**, *129*, 253.
(5) Cao, R. R.; Pope, S. B. *Combust. Flame* **2005**, *143*, 450.
(6) Griffiths, J. F. *Prog. Energy Combust. Sci.* **1995**, *21*, 25.
(7) Tomlin, A. S.; Turányi, T.; Pilling, M. J. In *Comprehensive Chemical Kinetics 35: Low-temperature Combustion and Autoignition*; Pilling, M. J., Ed.; Elsevier: Amsterdam, 1997; pp 293−437.
(8) Okino, M. S.; Mavrovouniotis, M. L. *Chem. Rev.* **1998**, *98*, 391.
(9) Bodenstein, M.; Lind, S. C. *Z. Phys. Chem., Stoechiom. Verwandtschaftsl.* **1906**, *57*, 168.
(10) Smooke, M. D., Ed. *Reduced Kinetic Mechanisms and Asymptotic Approximations for Methane-Air Flames*; Springer: Berlin, 1991; Vol. 384.
(11) Turányi, T.; Tomlin, A. S.; Pilling, M. J. *J. Phys. Chem.* **1993**, *97*, 163.
(12) Ren, Z.; Pope, S. B. *Combust. Flame* **2004**, *137*, 251.
(13) Ren, Z.; Pope, S. B. *Combust. Theory Modelling* **2006**, *10*, 361.
(14) Fraser, S. J. *J. Chem. Phys.* **1988**, *88*, 4732.
(15) Roussel, M. R.; Fraser, S. J. *J. Phys. Chem.* **1993**, *97*, 8316.
(16) Maas, U.; Pope, S. B. *Combust. Flame* **1992**, *88*, 239.
(17) Pope, S. B.; Maas, U. *Simplifying chemical kinetics: Trajectory-generated low-dimensional manifolds*; FDA 93-11; Cornell University: Ithaca, NY, 1993.
(18) Davis, M. J.; Skodje, R. T. *J. Chem. Phys.* **1999**, *111*, 859.
(19) Keck, J. C.; Gillespie, D. *Combust. Flame* **1971**, *17*, 237.
(20) Keck, J. C. *Prog. Energy Combust. Sci.* **1990**, *16*, 125.
(21) Lam, S. H.; Goussis, D. A. *Int. J. Chem. Kinet.* **1994**, *26*, 461.
(22) Gorban, A. N.; Karlin, I. V. *Chem. Eng. Sci.* **2003**, *58*, 4751.
(23) Gear, C. W.; Kaper, T. J.; Kevrekidis, I. G.; Zagaris, A. *SIAM J. Appl. Dynam. Syst.* **2005**, *4*, 711.
(24) Gear, C. W.; Kevrekidis, I. G. *J. Sci. Comput.* **2005**, *25*, 17.
(25) Davis, M. J. *J. Phys. Chem. A* **2006**, *110*, 5235.

(26) Davis, M. J. *J. Phys. Chem. A* **2006**, *110*, 5257.

(27) Skodje, R. T.; Davis, M. J. *J. Phys. Chem. A* **2001**, *105*, 10356.

(28) Singh, S.; Powers, J. M.; Paolucci, S. *J. Chem. Phys.* **2002**, *117*, 1482.

(29) Maas, U.; Pope, S. B. *Proc. Combust. Inst.* **1992**, *24*, 103.

(30) Maas, U.; Pope, S. B. *Proc. Combust. Inst.* **1994**, *25*, 1349.

(31) Lam, S. H. *The effect of fast chemical reactions on mass diffusion*; Report T1953-MAE; Princeton University: Princeton, NJ, 1992.

(32) Lam, S. H. *Combust. Sci. Technol.* **2007**, *179*, 767.

(33) Ren, Z.; Pope, S. B. *Combust. Flame* **2006**, *147*, 243.

(34) Ren, Z.; Pope, S. B.; Vladimirsky, A.; Guckenheimer, J. M. *Proc. Combust. Inst.* **2007**, *31*, 473.

(35) Yannacopoulos, A. N.; Tomlin, A. S.; Brindley, J.; Merkin, J. H.; Pilling, M. J. *Physica D* **1995**, *83*, 421.

(36) Goussis, D. A.; Valorani, M.; Creta, F.; Najm, H. N. *Progress in Comput. Fluid Dynam.* **2005**, *5*, 316.

(37) Strang, G. *SIAM J. Numer. Anal.* **1968**, *5* (3), 506.

(38) Ren, Z.; Pope, S. B. Transport-chemistry coupling in the reduced description of reactive flows. *Combust. Theory Modelling* **2007**, DOI: 10.1080/13647830701200000.

(39) Ren, Z.; Pope, S. B. *Proc. Combust. Inst.* **2005**, *30*, 1293.

(40) Tang, Q.; Xu, J.; Pope, S. B. *Proc. Combust. Inst.* **2000**, *28*, 133.

(41) Griffiths, J. F.; Sykes, A. *J. Chem. Soc., Faraday Trans.* **1989**, *85*, 3059.

(42) Johnson, B. R.; Scott, S. K. *J. Chem. Soc., Faraday Trans.* **1990**, *86*, 3701.

(43) Johnson, B. R. Ph.D. Thesis, Department of Chemistry, University of Leeds, 1991.

(44) Johnson, B. R.; Griffiths, J. F.; Scott, S. K. *Chaos* **1991**, *1*, 387.

(45) Scott, S. K. In *Comprehensive Chemical Kinetics 35: Low-temperature Combustion and Autoignition*; Pilling, M. J., Ed.; Elsevier: Amsterdam, 1997; pp 439−544.

(46) Hughes, K. J.; Turányi, T.; Clague, A.; Pilling, M. J. *Int. J. Chem. Kinet.* **2001**, *33*, 513.

(47) http://www.chem.leeds.ac.uk/Combustion/methane.htm.

(48) Caracotsios, M.; Stewart, W. E. *Comput. Chem. Eng.* **1985**, *9*, 359.

(49) Ren, Z.; Pope, S. B. Second-order splitting schemes for a class of reactive systems. *J. Comput. Phys.*, submitted for publication.

(50) Lu, T.; Ju, Y.; Law, C. K. *Combust. Flame* **2001**, *126*, 1445.

(51) Tang, Q.; Pope, S. B. *Proc. Combust. Inst.* **2002**, *29*, 1411.